Self-assembly and supramolecular isomerism in 1D Metal-Organometallic Networks based on transition metal assemblies from 1,1'-ferrocene-dicarboxylic acid and ancillary nitrogen heterocycle ligands

María L. Ospina-Castro,[a] Edward E. Ávila,[b*] Alexander Briceño,[c*] Andreas Reiber,[d] Leonardo C. Pacheco-Londoño[e] and Nataly J. Galan-Freyle[e]

[a] *Grupo de investigación Química Supramolecular Aplicada, Programa de Química, Universidad del Atlántico, Barranquilla, Colombia.*

[b]*Universidad Yachay Tech, Escuela de Ciencias Químicas e Ingeniería, Hda. San José, Urcuquí, Ecuador. Apartado postal: 100119. Tel: +593 6 2 999 500 ext. 2622; E-mail: eavila@yachaytech.edu.ec*

[c]*Laboratorio de Síntesis y Caracterización de Nuevos Materiales, Centro de Química, Instituto Venezolano de Investigaciones Científicas, San Antonio de Los Altos, Miranda, Venezuela. Fax: +58 212 5041320; Tel: +58 212 5041609; E-mail: aobriceno@gmail.com*

[d]*Laboratorio de la Interfase Inorgánica-Orgánica, Universidad de los Andes, Bogotá, Colombia.*

[e]*Life Science Research Center, Universidad Simón Bolívar, Barranquilla 080002, Colombia.*

Electronic Supplementary Information Content:

1 General information and materials.

All chemicals were commercially available and were purchased from Sigma-Aldrich as reagent grade quality and used without further purification. Elemental analysis was carried out on an EA1108 CHNS-O Fision Instrument.

2 Synthesis of compounds 1-7.

1,1'-ferrocenedicarboxylic acid (50.1 mg, 0.11 mmol) and 4,4'-bipy (52.1 mg, 0.33 mmol) were mixed with H_2O and the metallic acetate $M(OAc)_2$ according to the schematic diagram shown in Fig. S1. Then, these were heated in a Teflon-lined autoclave from 80 to 100 °C for three days. Good quality crystals were obtained.

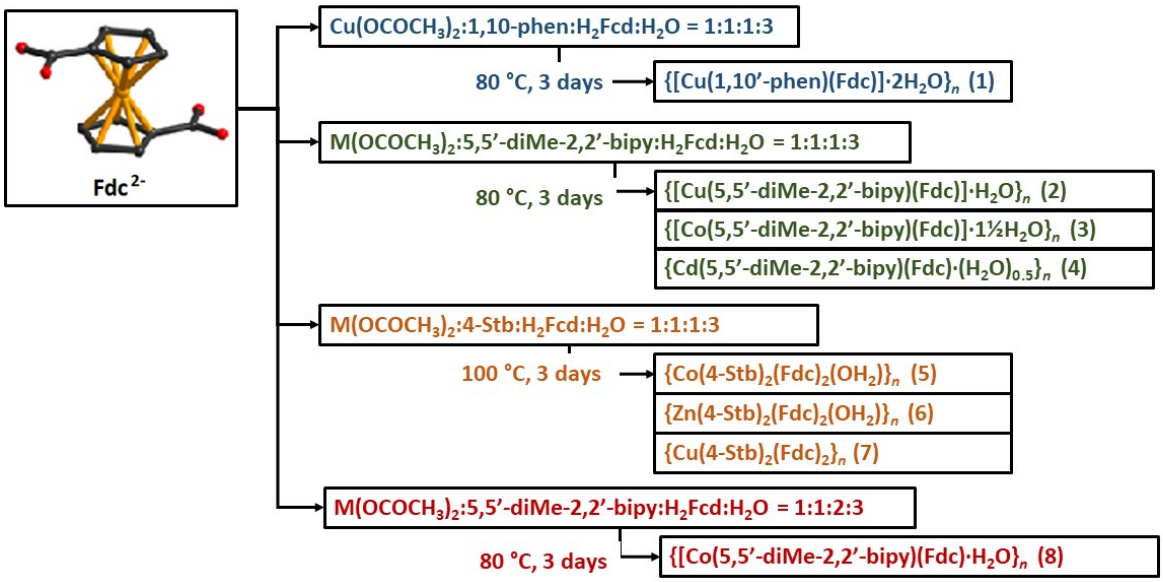

Fig. S1. Schematic reaction condition of MOMNs.

3 Crystal structure determination.

The single-crystal data collection was carried out on three different diffractometers. For the compounds **1**, **3** and **5** the data were collected on Rigaku AFC-7, Mercury II (Centro de Química, Instituto Venezuelano e Investigaciones Científicas, Miranda, Venezuela) at 298 (2) K with Mo-*K*α radiation. The single crystals were selected and mounted on a glass fiber. In the case, the compound **2** data were collected performed at 193 (2) K with an APEX II Bruker-AXS (Centre de Diffractométrie, Université de Rennes 1, France) with Mo-*K*α radiation. For last, compounds **4**, **6**, and **7** data were collected on an Agilent SuperNova, CrysAlis Pro, Oxford Cryojet, detector Atlas with Mo/Cu radiation (Universidad de Los Andes, Bogotá, Colombia). The single crystal was always coated in paratone oil once removed from the mother solution.

The data merging process was performed using the *CrystalClear, CrysAlisPro,* and *SCALAPACK* programs for source data of Rigaku AFC-7, Agilent SuperNova CrysAlisPro, Software System, Version 171.37.34, and APEX II Bruker-AXS, respectively.

Structure determinations were performed by dual-space iterative phasing algorithm[1] with the solving program SUPERFLIP,[2] that revealed all the non-hydrogen atoms. SHELXL-2018,[3,4,5] program was used to refine the structures by full-matrix least-squares based on F^2 with the use of SHELXLE program.[6] Most non-hydrogen atoms were refined with anisotropic displacement parameters. Hydrogen atoms were included in idealized positions and refined with isotropic displacement parameters. The SQUEEZE method was performed for

compounds **1** and **3** for addressing the solvent disorder issue.[7] In these compounds found that the solvent disorder issue to corresponds one molecule of water in both cases. Table S1 gives the crystallographic data for the derivatives **1** and **3** after its PLATON-SQUEEZE treatment. Table S1 shows crystallographic and refinement details, some selected bond distances and angles, and torsion angles are shown in Table S2. Table S3 displays hydrogen-bond geometry for compounds **1** - **2**. CCDC reference numbers CCDC 1830992, 1939225-1939233 contain the supplementary crystallographic data for derivatives **2**, **1**, **3-6**, respectively. These data can be obtained free of charge at www.ccdc.cam.ac.uk/conts/retreving.html or from the Cambridge Crystallographic Data Center, 12 union Road, Cambridge CB2 1EZ, UK; Fax: (internet.) + 44-1223-336-033; E-mail: deposit@ccdc.cam.ac.uk.

4 Powder X-ray diffraction patterns data.

The powder diffraction patterns data were collected with the powder X-ray diffractometer Bragg-Brentano geometry on Siemens, D5005 at the University of The Andes, Mérida, Mérida-Venezuela, with the powdered samples were mounted on the axis of the diffractometer and spun during measurements. This diffractometer is equipped with a monochromator of graphite. Data were collected for several minutes with Cu-Kα (λ = 1.54059 Å) anode focus length and fine, powered at 40 kV-30 mA. Additionally, for the data collection, a fixed slit and a divergence slit of 1 mm were used. A sample was made in a record of the maxima in the angular range of 10° to 100° in 2θ, using a step size of 0.02° and a counting time of 40 s per step.

5 FT-IR Measurement.

KBr pellets of the product compounds were used for IR data recording on a NICOLET MAGNA 560 spectrophotometer in the 400-4000 cm^{-1} region.

6 TGA-Measurement.

TGA measurements were performed on a Netzsch STA 409. The samples were prepared by loading into Alumina´s crucibles in quantities between 8 - 10.0 mg for each one. Test were carried-out by heating the sample from 30 to 600°C at a rate of 10 °C min^{-1} under a nitrogen atmosphere.

7 Powder X-ray Diffraction Analysis

The peak shapes were modeled using the split pseudo-Voigt peak shape function. The background was initially determined automatically and then modeled using the B-spline function. Restraints on distances and angles bond do not were applied. However, these were taken in the refinement fixed rigid model. The global isotropic atomic displacement parameters were refined as one overall U_{iso} for all atoms starting from a value of 0.03 $Å^2$. At this point, the Figures of Merit obtained for the WPPF refinement were: R_p = 0.068, R_{wp} = 0.087, R_{exp} = 0.070, and χ^2 = 1.57.

Structure Refinement by whole powder pattern fitting (WPPF) Table S5 shows the refined parameter by whole powder pattern fitting (WPPF)[8-10] methodology using *SmartLab Studio* 4.3 program.[11] The non-hydrogen atoms crystallographic positions for 2´-Co(II) (**8**), 3- Co(II), and Mc-Co(II) were obtained of **2**, **3**, and **Mc-Co(II)** from CSD Code: HUGSAF. The hydrogen atoms were token as riding models.

8 Differential pulse voltammetry.

Differential pulse voltammetry studies were carried out on a Voltalab 80 (Radiometer Analytical) using a three-electrode configuration consisting of a Pt working electrode, a Pt auxiliary electrode, and a commercially available Ag/AgCl electrode as a reference with a pure Ar gas inlet and outlet. The

measurements were performed in DMF solution containing Tetrabutylammonium hexafluorophosphate ($TBAPF_6$) (0.1 M) as supporting electrolyte, with 50 ms pulses. The potential from + 0.3 to +1.1 V was scanned at a scan rate of 20 mVs^{-1} and with 50 ms pulses.

Table S1. Experimental details for X-ray diffraction collected data and structural refinement. Crystal data and structure refinement for compounds **1-7.**

	Compound 1	**Compound 2**	**Compound 3**	**Compound 4**	**Compound 5**	**Compound 6**	**Compound 7**
Crystal data	**Cu**	**Cu**	**Co**	**Cd**	**Co**	**Zn**	**Cu**
Chemical formula	$C_{24}H_{16}CuFeN_2O_4 \cdot H_2O$	$C_{24}H_{20}CuFeN_2O_4 \cdot H_2O$	$C_{24}H_{24}CoFeN_2O_6 \cdot 1.5H_2O$	$C_{24}H_{20}CdFeN_2O_4 \cdot ½H_2O$	$C_{38}H_{32}CoFeN_2O_5$	$C_{38}H_{32}ZnFeN_2O_5$	$C_{38}H_{32}CuFeN_2O_4$
M_r	533.79	537.82	551.23	577.68	711.43	717.87	698.03
Crystal system, space group	Monoclinic, *P2₁/c* (No. 14)	Monoclinic, *P2₁/c* (No. 14)	Orthorhombic, *Pnna* (No. 62)	Monoclinic, *P2₁/c* (No. 14)	Triclinic, *P-1* (No. 2)	Triclinic, *P-1* (No. 2)	Triclinic, *P-1* (No. 2)
Temperature (K)	293 (2)	193 (2)	293 (2)	100 (2)	293 (2)	100 (2)	100 (2)
a, *b*, *c* (Å)	5.707 (10), 25.67 (5), 14.37 (3)	5.8675 (5), 20.1101 (16), 18.3448 (15)	23.977 (11), 12.069 (5), 8.344 (4)	5.9086 (3), 16.8542 (8), 21.1889 (12)	10.241 (6), 12.460 (9), 13.234 (9)	10.2015 (8), 12.2977 (6), 13.0982 (5)	10.7394 (4), 12.0118 (5), 12.6687 (3)
α, β, γ (°)	90, 97.07 (5), 90	90, 98.242 (9), 90	90, 90, 90	90, 92.684 (5), 90	106.27 (3), 91.968 (17), 93.26 (2)	105.694 (4), 92.706 (5), 93.349 (5)	77.694 (3), 78.073 (3), 79.980 (3)
V (Å³)	2089 (7)	2140.4 (3)	2414.5 (19)	2107.78 (19)	1616.2 (19)	1575.87 (16)	1547.73 (10)
Z	4	4	4	4	2	2	2
Radiation type	Mo *K*α	Mo *K*α	Mo *K*α	Cu *K*α	Mo *K*α	Cu *K*α	Cu *K*α
μ (mm⁻¹)	1.75	1.712	1.33	13.92	1.01	5.03	4.97
Crystal size (mm)	0.60 × 0.30 × 0.25	0.10 x 0.07 x 0.04	0.60 × 0.30 × 0.25	0.14 × 0.06 × 0.06	0.40 × 0.35 × 0.25	0.08 × 0.08 × 0.08	0.20 × 0.18 × 0.08
Data collection							
Diffractometer	Rigaku AFC7 Mercury, Mercury	Bruker AXS, Apex II	Rigaku AFC7 Mercury, Mercury	SuperNova, Dual, Cu at zero, Atlas	Rigaku AFC7 Mercury, Mercury	SuperNova, Dual, Cu at zero, Atlas	SuperNova, Dual, Cu at zero, Atlas
Absorption correction	Multi-scan methodology.	Semi-empirical from equivalents	Multi-scan methodology.	Multi-scan methodology.	Multi-scan methodology.	Multi-scan methodology.	Multi-scan methodology.
No. of measured, independent and observed [$I > 2\sigma(I)$] reflections	9892, 3238, 2092	11779, 2476, 1810	17225, 1964, 1449	29826, 4239, 3885	16238, 5193, 2325	21382, 6238, 5988	75556, 5597, 5385
Rint	0.065	0.090	0.067	0.047	0.148	0.035	0.063
$(\sin \theta/\lambda)_{max}$ (Å⁻¹)	0.627	0.703	0.627	0.624	0.629	0.624	0.600
Refinement							
$R[F^2 > 2\sigma(F^2)]$, $wR(F^2)$, S	0.060, 0.150, 1.14	0.0408, 0.0959, 1.093	0.061, 0.118, 1.14	0.032, 0.080, 1.06	0.093, 0.178, 1.07	0.037, 0.101, 1.05	0.032, 0.087, 1.06
No. of reflections	3238	5267	1964	4239	5193	6238	5597
No. of parameters	305	307	159	312	401	425	453
No. of restraints	0	1	2	15	0	0	384
H-atom treatment	H-atom parameters constrained	H atoms constrained refinement	H-atom parameters constrained	H-atom parameters constrained	H-atom parameters constrained	H-atom parameters constrained	H-atom parameters constrained
$\Delta\rho_{max}$, $\Delta\rho_{min}$ (e Å⁻³)	0.43, −0.46	0.40, −0.49	0.28, -0.53	0.55, -0.63	0.45, -0.53	0.73, −0.81	0.89, −0.46

Computer programs: *CrystalClear* (Rigaku/MSC Inc., 2005), *SUPERFLIP* (Palatinus & Chapuis, 2007), *SHELXL2018*/3 (Sheldrick, 2018), *DIAMOND* (Brandenburg, 1998), *PLATON* (Spek, 2003) & *publCIF* (Westrip, 2010).

Table S2. Selected bond distances, angles, and torsion angle for compounds **1-7**.

	Compound 1	Compound 2	Compound 3	Compound 4$	Compound 5	Compound 6	Compound 7$
Distances (Å)	**Cu**	**Cu**	**Co**	**Cd**	**Co**	**Zn**	**Cu**
M1—N1	2.018(6)	2.0004(1)	2.086(5)	2.352(3)	2.170(7)	2.171(2)	2.050(4)/1.82(3)
M1—N2	2.018(6)	1.9890(1)	2.086(5)^{i}	2.284(4)	2.189(8)	2.192(2)	2.074(4)/1.78(3)
M1—O1	1.956(5)	1.9508(1)	2.129(4)	2.367(2)	2.017(6)	2.012(2)	1.974(1)
M1—O2	2.551(7)	2.6430(1)	2.129(4)^{i}	2.321(3)	3.252(7)	3.193(2)	-
M1—O3	1.952(5)	1.9421(1)	2.152(4)	2.301(6)/2.13(1)	2.161(7)	2.159(2)	1.940(1)
M1—O4	2.468(7)	2.5670(1)	2.152(4)^{i}	2.408(5)/3.152(7)	2.153(6)	2.201(2)	2.313(2)
M1—O1W	-	-	-	2.362(6)	2.082(6)	2.078(2)	-
M1—C6	2.576(8)	2.5793(2)	2.4850(6)	2.69(1)/2.97(2)	2.95(1)	2.922(2)	2.637(2)
M1—C12	2.538(9)	2.6175(1)	2.485(6)^{i}	2.691(3)	2.48(1)	2.513(2)	-
C6—O1	1.294(8)	1.2371(1)	1.269(7)	1.25(1)/1.26(2)	1.26(1)	1.274(3)	1.276(3)
C6—O2	1.224(8)	1.2880(1)	1.269(7)^{i}	1.27(2)/1.25(1)	1.27(1)	1.253(3)	1.247(2)
C12—O3	1.281(8)	1.2303(1)	1.268(8)	1.251(4)	1.25(1)	1.263(3)	1.279(3)
C12—O4	1.242(9)	1.2884(1)	1.268(8)^{i}	1.264(4)	1.29(1)	1.275(3)	1.239(3
Angles (°)	**Cu**	**Cu**	**Co**	**Cd**	**Co**	**Zn**	**Cu**
N1—M1—N2	82.010(231)	81.505(3)	77.3(2)^{i}	71.2(1)	178.1(3)	176.569(68)	177.9(1)/176(1) 173.0(9)/169(1)
N1—M1—O1	102.19(5)	102.923(3)	87.8 (2)^{i}	90.29(9)	89.3(3)	91.185(65)	92.3(1)/93(1)
N1—M1—O2	93.88(5)	94.141(4)	94.2(2)^{i}	90.0(2)/91.8(3)	-	-	-
N1—M1—O3	163.82(5)	165.544(4)	139.2(2)^{i}	143.3(2)	86.1(3)	87.14(6)	89.6(1)/87.7(1)
N1—M1—O4	94.47(4)	111.473(3)	119.2(2)^{i}	100.1(1)/98.3(1)	89.0(3)	86.83(7)	94.7(1)/101(1)
N1—M1—O1W	-	-	-	141.6(2)	86.5(3)	85.67(7)	-
N1—M1—C6	88.9(2)	99.584(3)	114.9(2)^{i}	-	-	-	-
N1—M1—C12	138.3(2)	138.302(4)	109.4(2)^{i}	117.1(1)	86.4(3)	85.59(7)	-
C12—M1—O1	100.9(2)	116.156(3)	125.5(2)^{i}	134.4(1)	131.1(3)	130.63(6)	-
C12—M1—O2	130.6(2)	96.307(3)	110.3(2)^{i}	99.1(2)			
C12—M1—O1W	-	-	-	99.5(2)	131.2(3)	129.09(7)	-
O1—M1—O1W	-	-	-	98.7(2)/86.7(3)	97.0(2)	99.960(6)	-
O1—M1—O3	96.2(2)	59.51(8)	61.4(1)^{i}	91.2(2)/105.0(3)	-	-	159.2(6)
O1—M1—O4	102.2(2)	153.9(1)	146.5(2)^{i}	105.5(2)/108.7(3)	-	-	90.0(6)
O3—M1—O4	58.3(2)	121.9(3)	99.9(1)^{i}	55.67(8)	-	-	115.6(6)
Torsion angle (°)							
C6—Cg1—Cg2—C12	−38.5(2)	−31.8(5)					

Symmetry codes: (i) x, $\frac{1}{2}$–y, $\frac{3}{2}$ – z, for **3** in *Pnna.*

Table S3. Hydrogen-bond geometry (Å, °) for compounds **1-7**.

D—H···A	D—H/Å	H···A/Å	D···A/Å	D—H···A/°
Compound 1				
O1W—H1W···O1	0.90(2)	1.98(2)	2.867(2)	167(2)
C5—H5···O2	0.9500	2.5700	3.342(2)	139.00
C9—H9···O1W	1.0000	2.4400	3.322(2)	147.00
Compound 2				
O1W—H1W···O1	0.92(2)	1.99(2)	2.893(3)	167(4)
C5—H5···O2	0.95	2.39	3.084(4)	130.00
C9—H9···O1W	1.00	2.51	3.339(4)	141.00
Compound 3				
Ow1—Hw1B···O2^{iii}	0.8500	2.0000	2.771(8)	150.00
Symmetry code: (iii) −x+1, y+1/2, z−1/2.				
Compound 3$^{\#}$				
Ow1—H1wA···O2^{i}	1.0000	1.6700	2.6756	175.00
Ow2—H2wA···Ow2^{v}	0.9800	2.3700	2.9618	118.00
(i) x, −y+3/2, −z+5/2; (v) −x+5/2, −y+1, z.				
Compound 4				
O1W—H1WA···O3A^{iii}	0.8700	2.5600	3.119(8)	123.00
O1W—H1WA···O4A	0.8700	1.7600	2.231(7)	111.00
O1W—H1WA···O4B	0.8700	1.9600	2.646(9)	134.00
O1W—H1WB···O1^{iii}	0.8700	1.9700	2.713(6)	142.00
Symmetry codes: (iii) x−1, y, z; (iv) x+1, −y+3/2, z−1/2; (v) x+1, y, z; (vi) −x+1, y−1/2, −z+3/2; (vii) −x, y−1/2, −z+3/2.				
Compound 5				
Ow1—H1W1···O2	0.9000	1.7700	2.646(9)	166.00
Ow1—H1W2···O4^{iii}	0.7200	1.9900	2.701(9)	170.00
C19—H19···O3^{iv}	0.9300	2.5200	3.384(15)	156.00
C27—H27···O2^{iii}	0.9300	2.6000	3.481(10)	159.00
Symmetry codes: (iii) −x+2, −y+1, −z; (iv) −x+2, −y+1, −z+1.				
Compound 6				
Ow1—H1W1···O2	0.8600	1.9100	2.650(2)	142.00
Ow1—H1W2···O4^{iii}	0.9600	1.7300	2.667(2)	163.00
C19—H19···O3^{iv}	0.9300	2.4400	3.289(3)	152.00
C27—H27···O2^{iii}	0.9300	2.4900	3.387(3)	163.00
Symmetry codes: (iii) −x+2, −y+1, −z; (iv) −x+2, −y+1, −z+1.				
#: These values were taken of calculation all by Platon from solid-state structure DFT theoretical calculation.				

Table S4. Half-wave potential ($E_{1/2}$) of the polymers **1-7**.

Polymer	$E_{1/2}$
1	0.91
2	0.88
3	0.89
4	0.92
5	0.89
6	0.94
7	0.90

Table S5. Experimental Details and Crystallography Refinement.

	2′-Co(II)	**3-Co**	**Mc-Co(II)[#]**
Crystal Data	**8**	**3**	**MC**
	$C_{24}H_{20}CoFeN_2O_5$	$C_{24}H_{26}CoFeN_2O_7$	$C_{48}H_{44}Co_2Fe_2N_4O_{10}$
Crystal system	Monoclinic	Orthorhombic	Monoclinic
Space group	$P2_1/c$ (N°14)	*Pnna* (N°52)	$P2_1/n$ (N°14)
Z	4	4	4
a/Å, *b*/Å, *c*/Å,	6.34(3), 15.31(5), 23.14(9)	23.938(5), 12.057(2), 8.3329(16)	13.0422(8), 11.2110(17), 15.3329(11)
α/°, β/°, γ/°	90, 84.1(3), 90	90, 90, 90	90, 106.986(7), 90
Volume/Å³	2232(14)	2405.0(8)	2144.1(4)
Calc. density/(g/cm³)	1.65004	1.572	1.97236
μ/(cm²/g)	71.268	67.367	1.491
M_r/(g/mol)	496.43	569.25	1066.44
Molar ratio/mol%	6.8(3)	82.9(9)	10.3(10)
Concentration, wt%	17.4(13)	72.9(12)	9.8(6)
Data collection			
Diffractometer	Panalytical, X'Pert, INTEVEP, Los Teques, Venezuela.		
Data preparation method	Specimen mounting: aluminum sample holder; mode: reflection; scan method: step		
Absorption correction	None		
2θ (°)	$2\theta_{min}$ = 4.95, $2\theta_{max}$ = 59.98.00, $2\theta_{step}$ = 0.02		
Refinement			
Refinement on	Intensity		
R factors and goodness of fit	R_p = 0.068, R_{wp} = 0.087, R_{exp} = 0.070; χ^2 = 1.570		
Excluded region(s)	None		
Profile function	Split pseudo-Voigt function		
$(\Delta/\sigma)_{max}$	0.40		

[#] Mc-Co(II): This corresponds to CSD Code: HUGSAF. M. L. O. Castro, A. Briceño, T. González, A. Reiber, G. Jorge, M. H. Duran, 2015, Inorg. Chim. Acta, 432, 275.

Table S6. Percentages of mass loss and transition temperatures for each compound were obtained from TGA.

Compound	1st Transition			2nd Transition		3rd Transition	
	m/m, %		t_t, °C	m/m, %	t_t, °C	m/m, %	t_t, °C
	Calc.	Obs.					
1	3.37	3.0	170.0	33.0	232.0		
2	3.34	3.0	123.0	30.0	243.0	59.0	402.0
3	4.98	5.0	198.0	-	-	73.0	425.0
4	1.56	8.0	100.9			40.0	358.0
5	2.53	2.70	174.0	-	-	54.0	325.0
6	2.51	2.60	-	3.0	217.0	41.0	301.0
7	-	-	-	-	-	61.0	324.0

-: This represents the mass loss transitions not observed according to the number of water molecules into the crystalline structure.

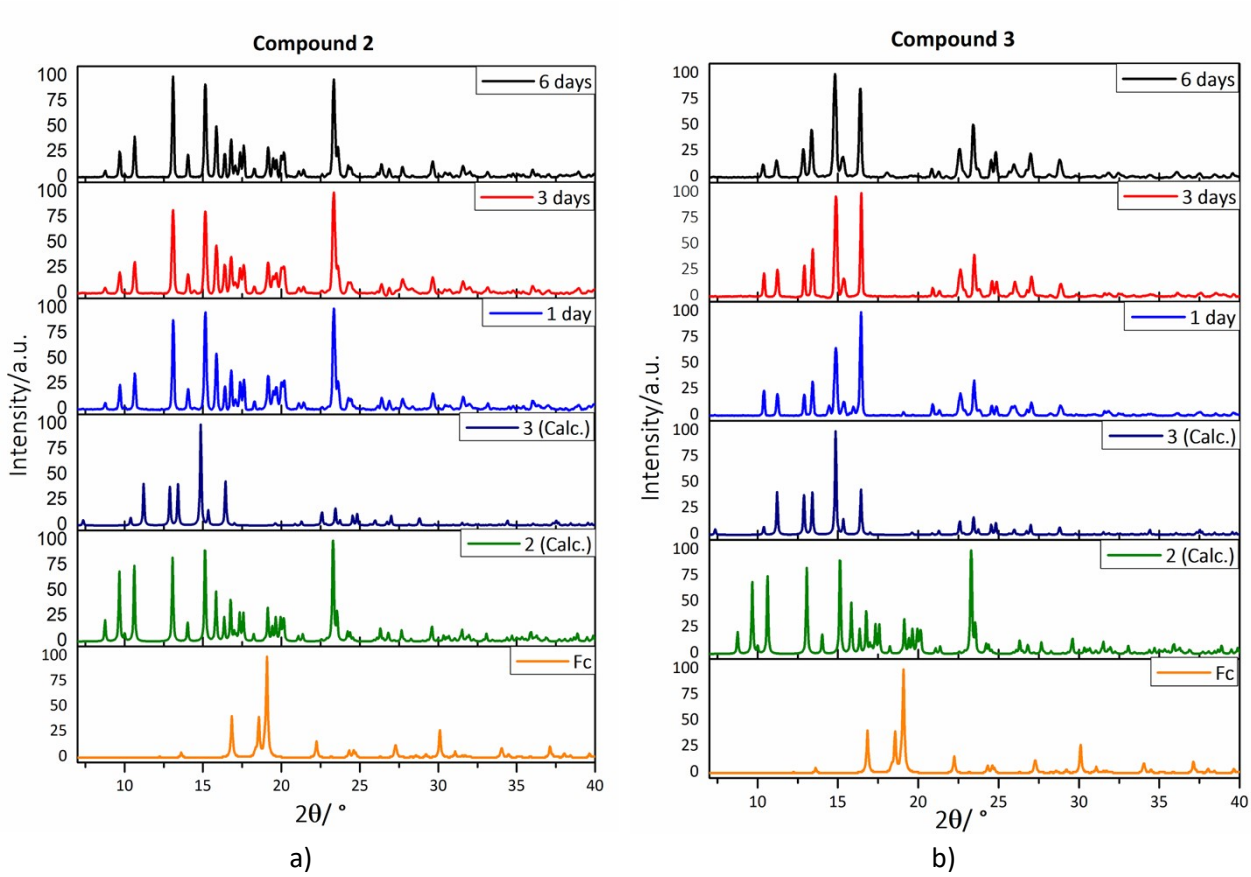

Fig. S2. Powder patterns for compounds **2** and **3** experimental (exp.) and calculated (calc.). Furthermore, the powder diffraction patterns include of the starting ligands 5,5'-diMe-2,2'-bipy (5,5'-dimethyl-2,2'-bipyrine) and Fc (1,1'-ferrocenedicarboxylic acid).

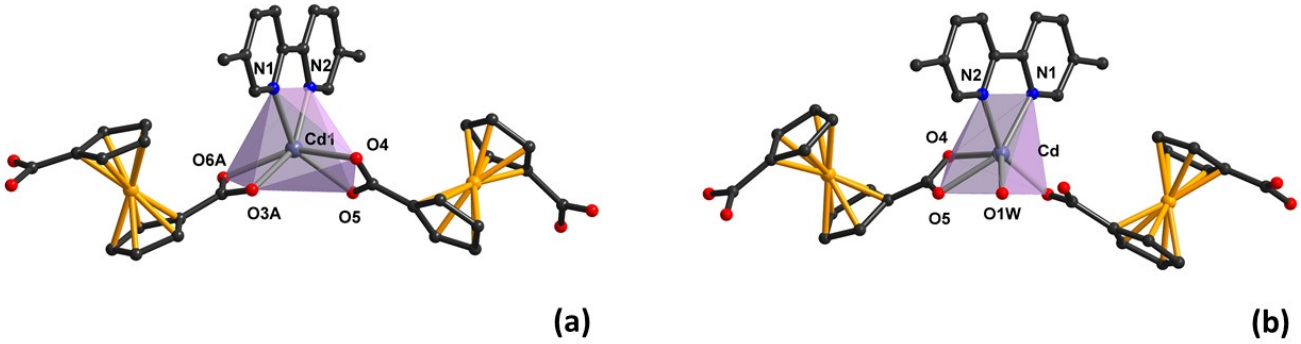

Fig. S3. Comparative representation of coordination spheres surrounded of Cd(II) ion, showing disorder between bidentade carboxylate mode (a) and water coordination and monodentade carboxylate (b).

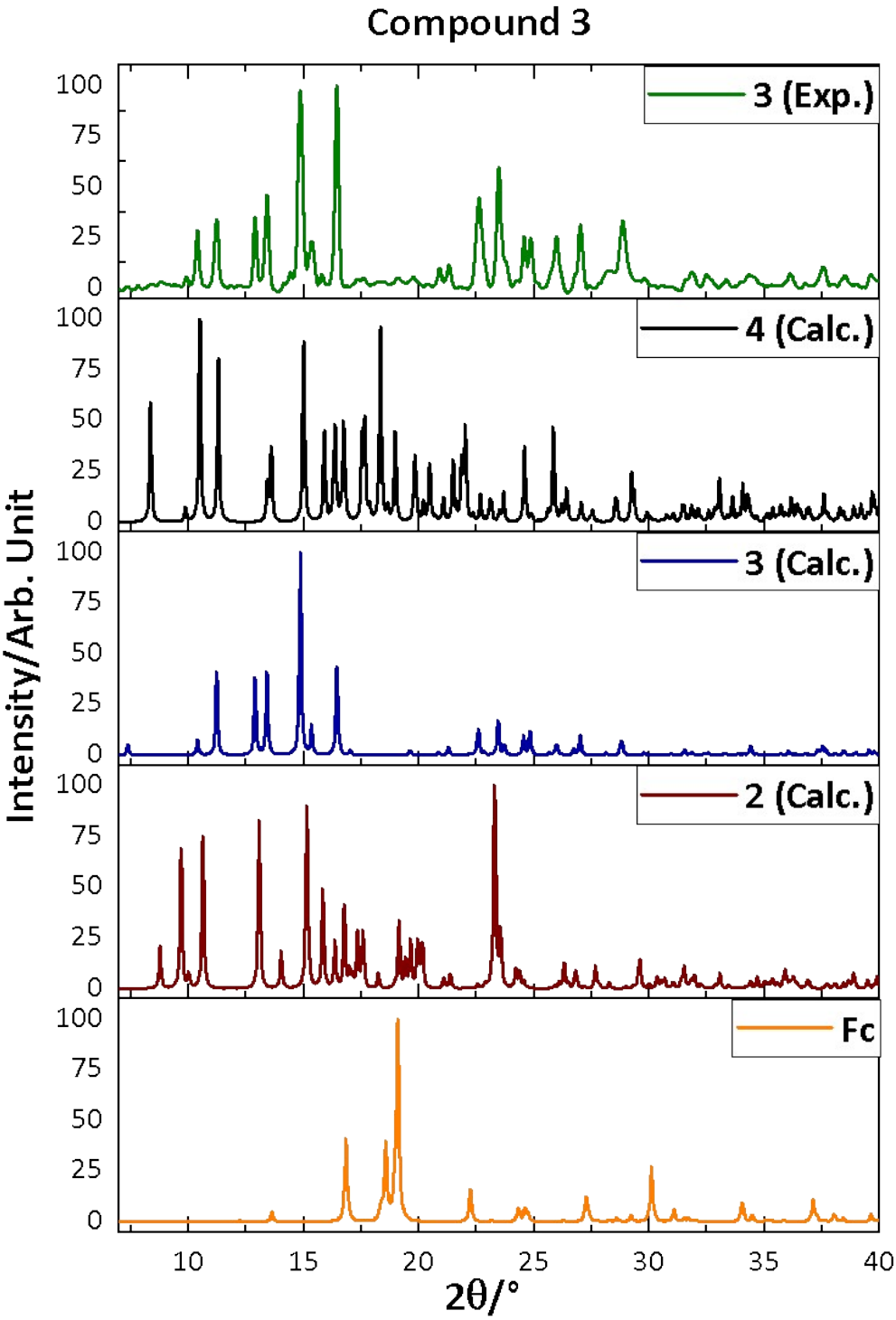

Fig. S4. Comparative powder patterns calculated (**2**, **3**, and **4**) and experimental for compound **3**. The powder diffraction pattern calculated of the starting ligand Fc is also included (Fc = 1,1'-ferrocenedicarboxylic acid).

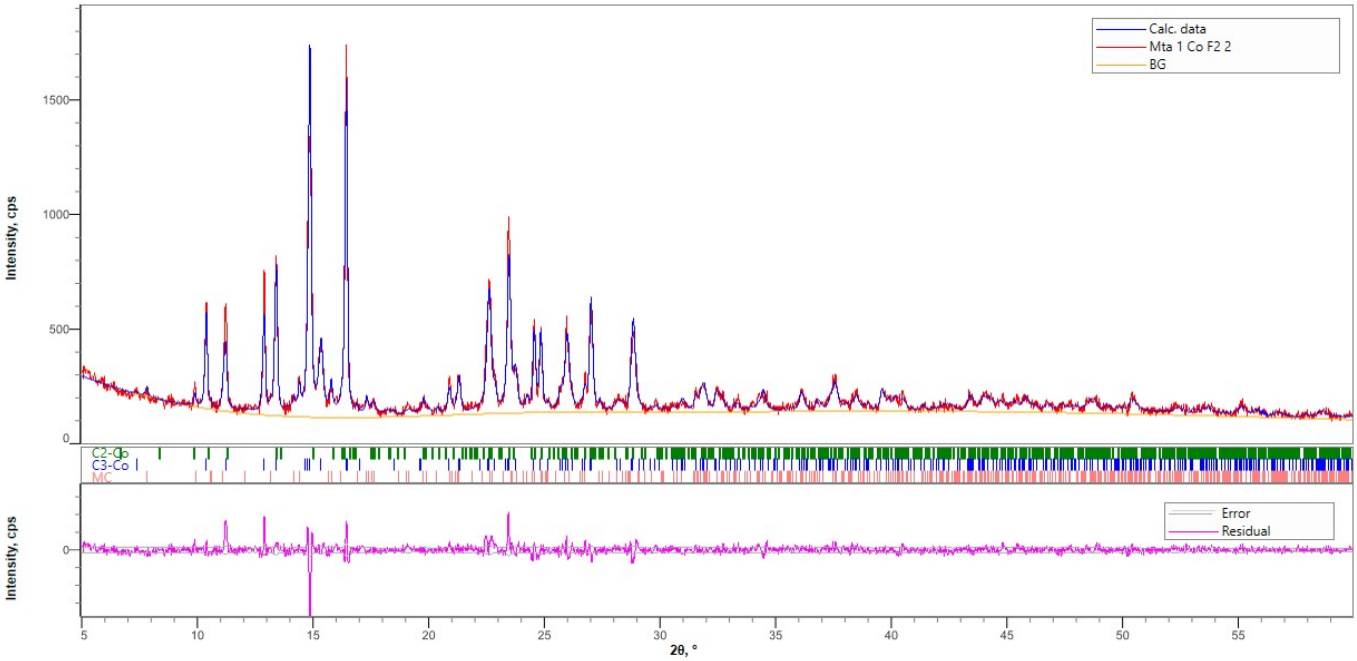

(a)

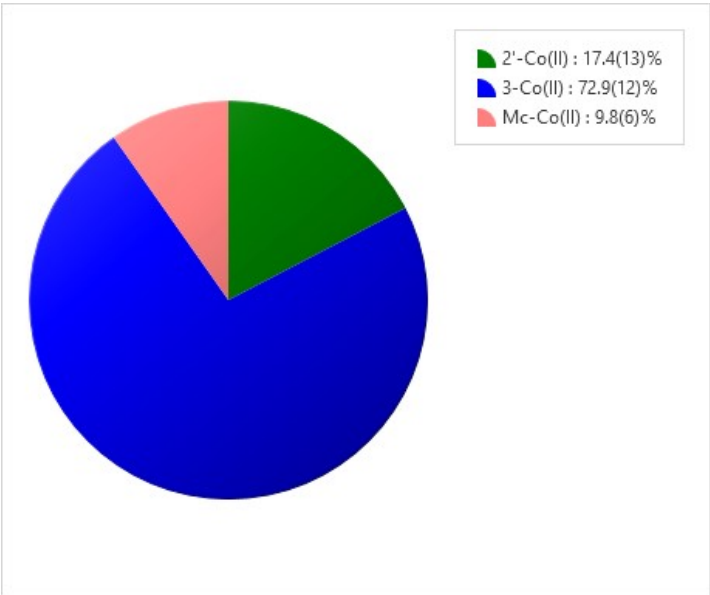

(b)

Fig. S5. Final Rietveld plot showing the observed, calculated pattern and differences for the **2´-Co(II)**, **3-Co(II)**, and **Mc´-Co(II)** phase mixtures. The Bragg reflections for each phase are labeled on the left (a). Additionality, the (a) shows the residual and error produced by Rietveld Refinement On the order hand, (b) is showing the phase ratio percentage found from the Rietveld refinement.

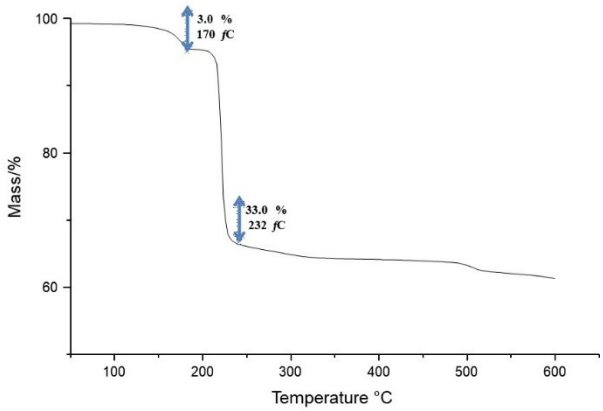

(a) Compound 1

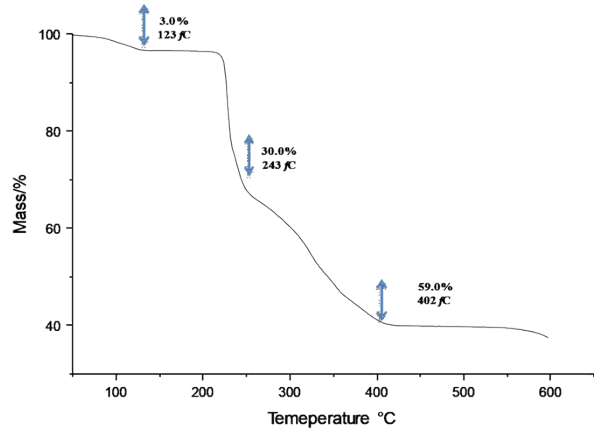

(b) Compound 2

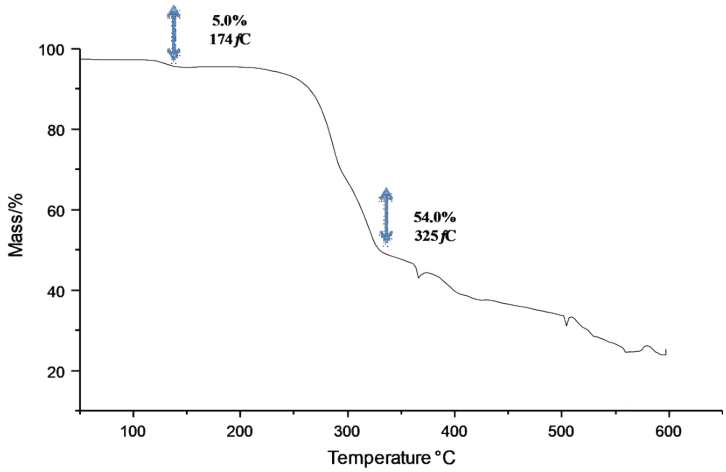

(c) Compound 3

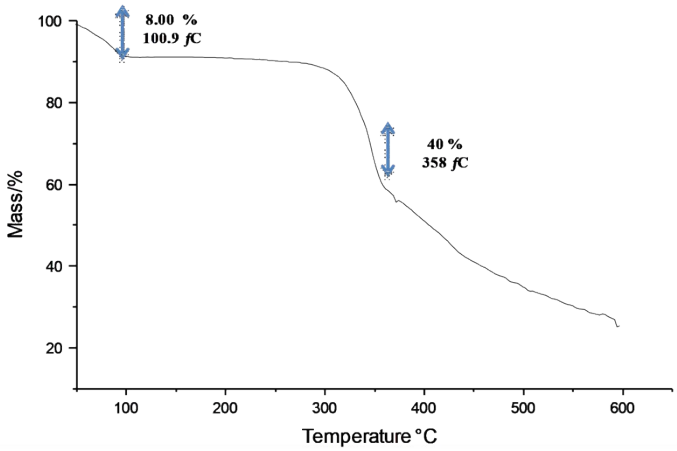

(d) Compound 4

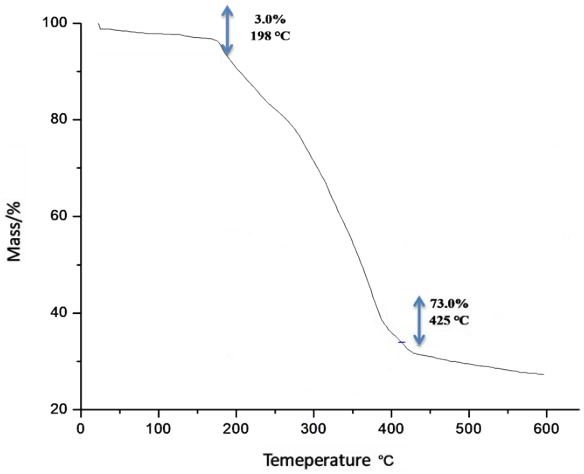

(e) Compound 5

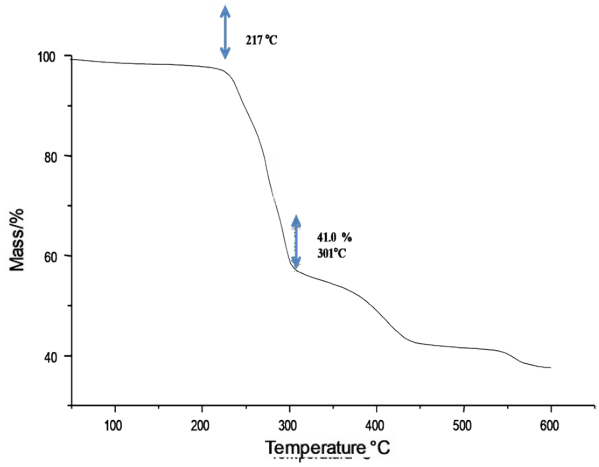

(f) Compound 6

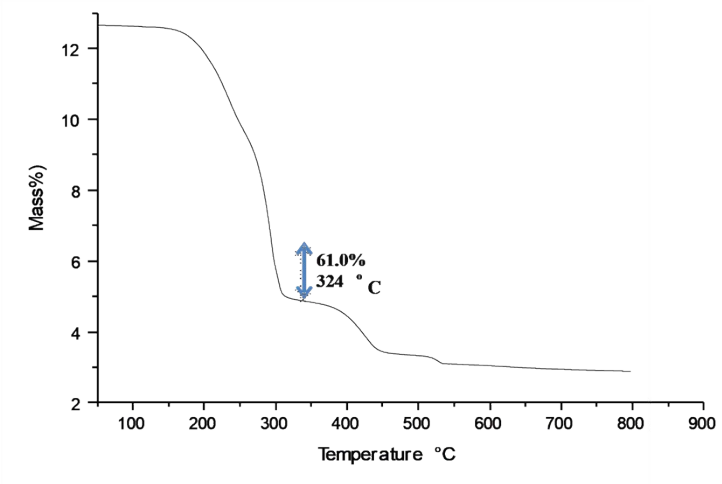

(g) Compound 7

Fig. S6. TGA curves for compound 1-7.

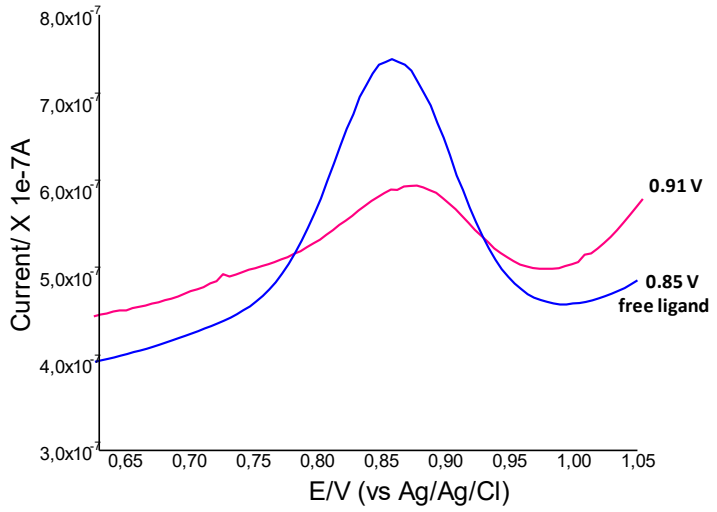

(a) Compound 1

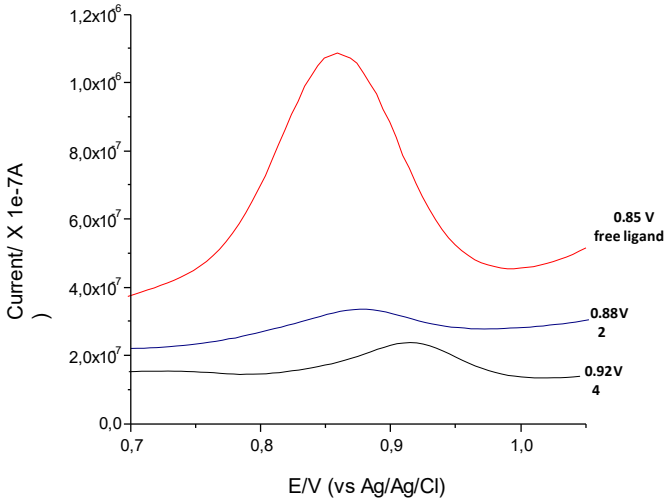

(b) Compound 2 and 4

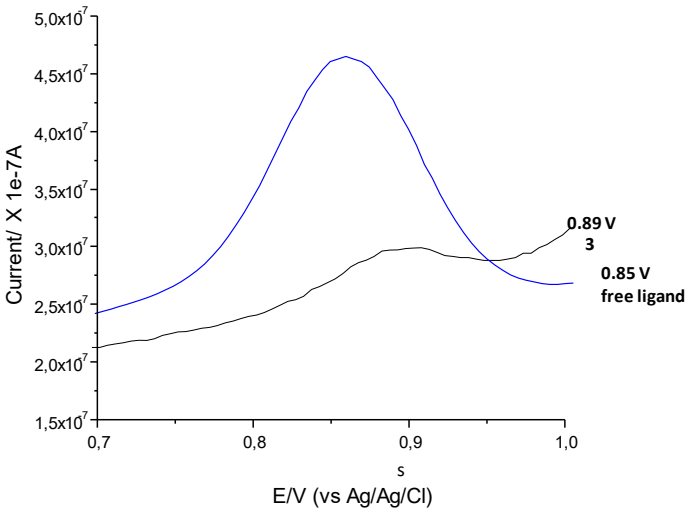

(c) Compound 3

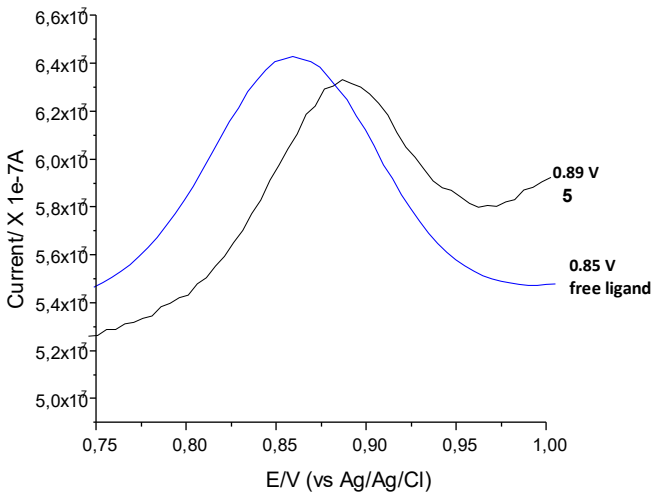

(d) Compound 5

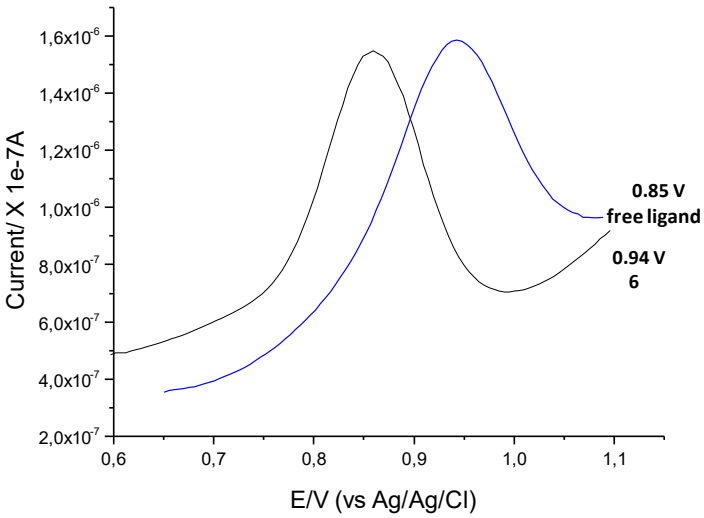

(e) Compound 6

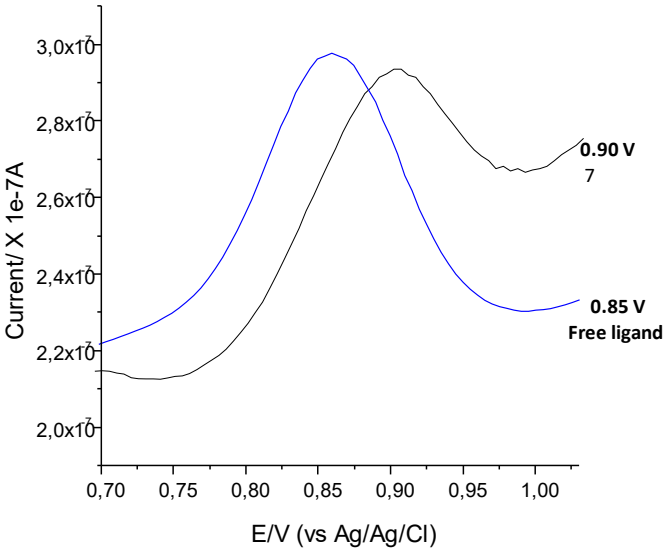

(f) Compound 7

Fig. S7. Differential pulse voltammograms (DPV) showing graphs for compounds **1**-**7** and 1,1'-ferrocenedicarboxylic acid, dissolved at a concentration of 1.0×10^{-3} M in DMF 0.1 M. The voltammograms were carried out at a scanning rate of 20 mVs^{-1} (vs. Ag/AgCl).

(a)

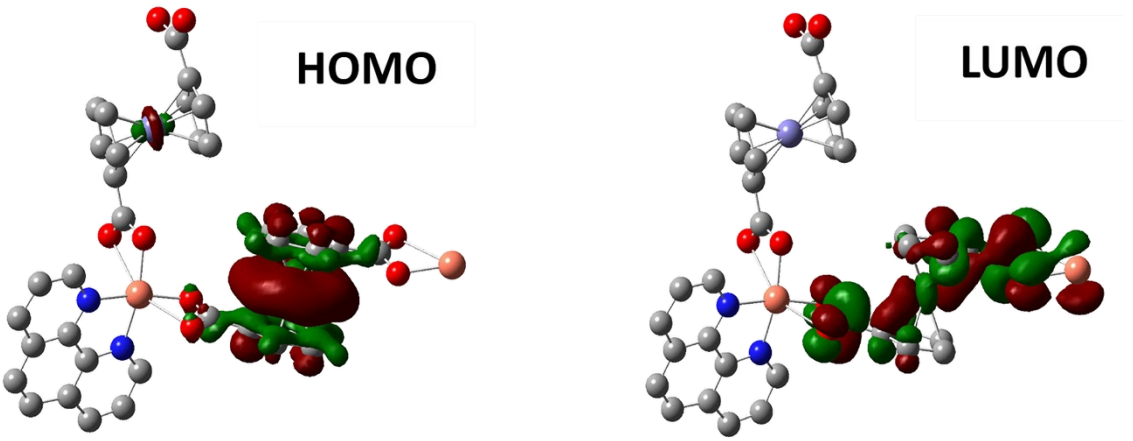

(b)

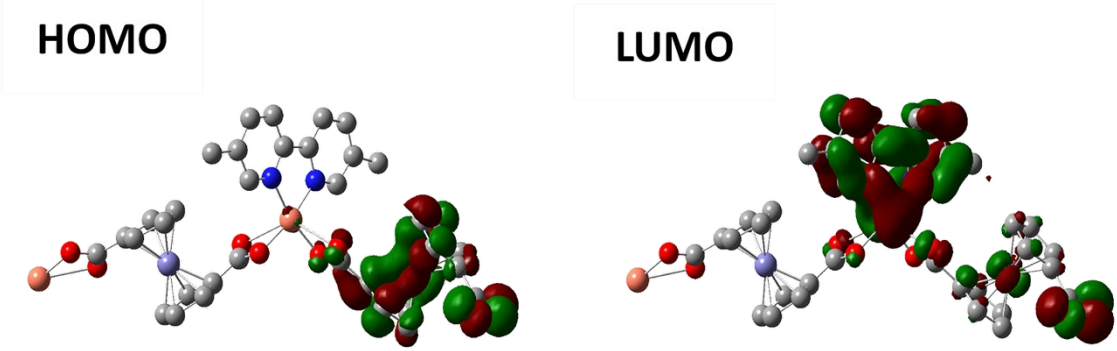

(c)

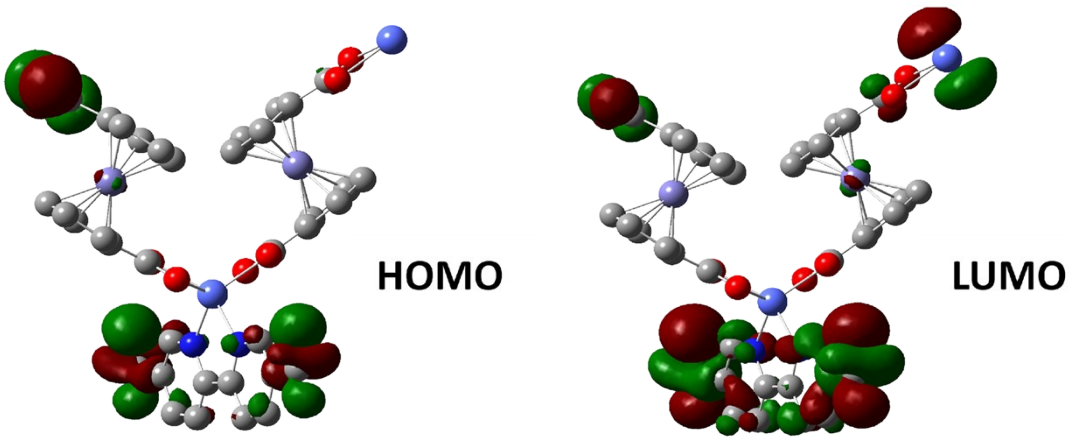

(d)

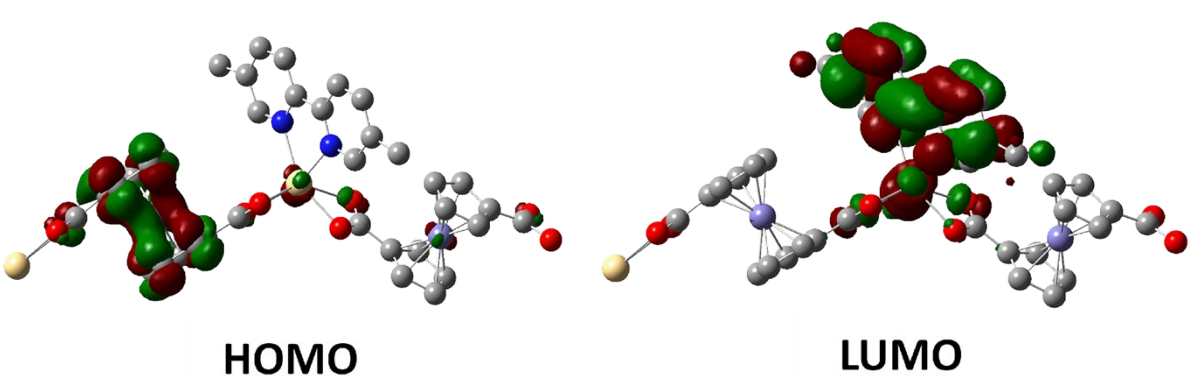

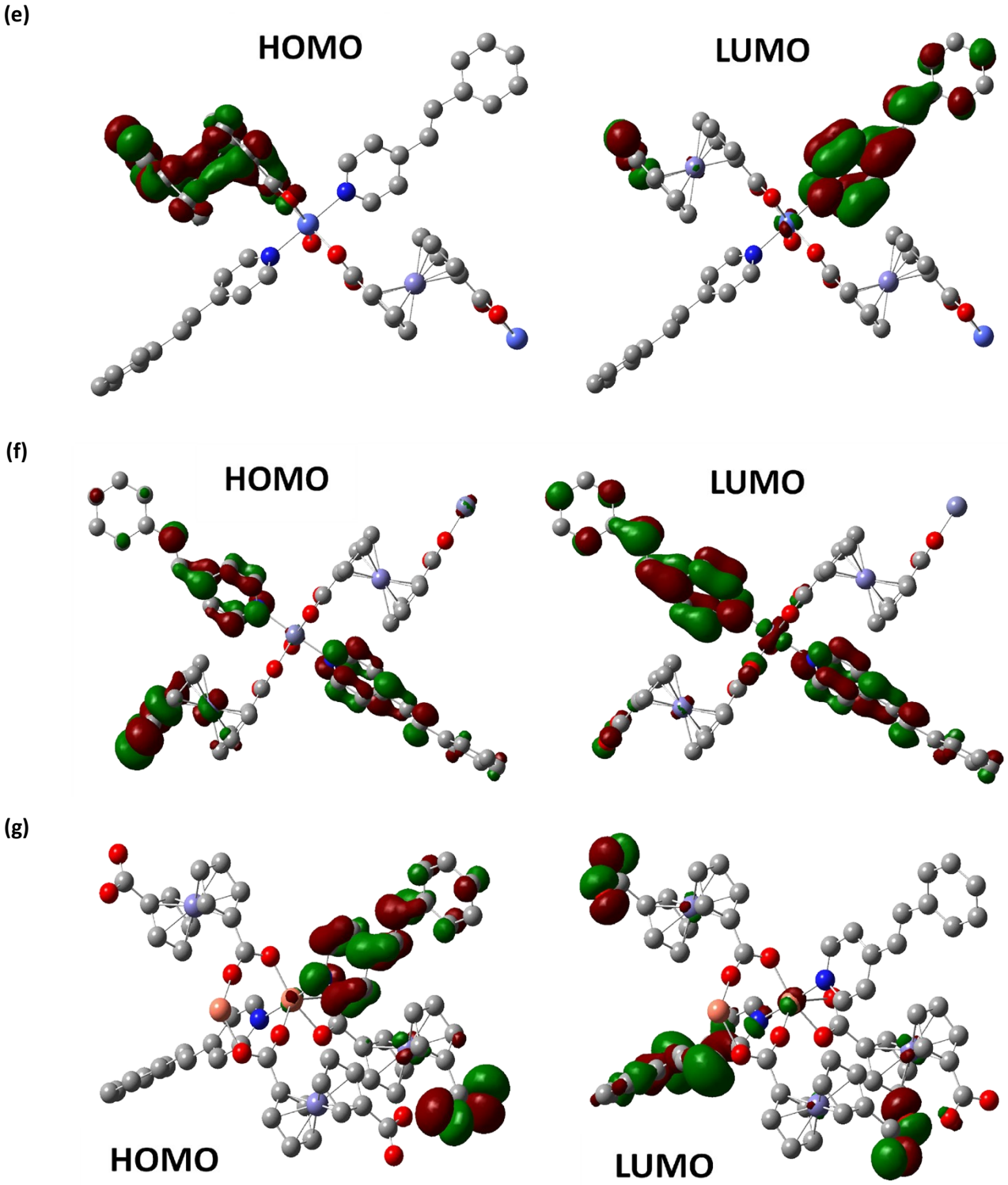

Fig. S8. Occupied Molecular Orbital (OMO) for the complex polymers were lowest that Fdc^{2-} anion this is indicated for compounds **1-7**.

9. Bibliographic Reference for ESI.

1 L. Palatinus, The charge-flipping algorithm in crystallography, *Acta Crystallogr. Sect. B Struct. Sci. Cryst. Eng. Mater.*, 2013, **69**, 1–16.

2 L. Palatinus and G. Chapuis, *SUPERFLIP* a computer program for the solution of crystal structures by charge flipping in arbitrary dimensions, *J. Appl. Crystallogr.*, 2007, **40**, 786–790.

3 G. M. Sheldrick, A short history of SHELX., *Acta Crystallogr. A.*, 2008, **64**, 112–22.

4 G. M. Sheldrick, Crystal structure refinement with SHELXL, *Acta Crystallogr. Sect. C Struct. Chem.*, 2015, **71**, 3–8.

5 G. M. Sheldrick, User guide to crystal structure refinement with SHELXL, DOI:10.1107/S2053229614024218.

6 C. B. Hübschle, G. M. Sheldrick and B. Dittrich, ShelXle: A Qt graphical user interface for SHELXL, *J. Appl. Crystallogr.*, 2011, **44**, 1281–1284.

7 A. L. Spek, PLATON SQUEEZE: a tool for the calculation of the disordered solvent contribution to the calculated structure factors, *Acta Crystallogr. Sect. C Struct. Chem.*, 2015, **71**, 9–18.

8 Rietveld, H. M. (1969). *J. Appl. Cryst*., 1969, **2**, 65–71.

9 Toraya, H., Whole-Powder-Pattern Fitting Without Reference to a Structural Model: Application to X-ray Powder Diffractometer Data, *J. Appl. Cryst*., 1986, **19**, 440-447.

10 Toraya, H. Applications of Whole-Powder-Pattern Fitting Technique in Materials Characterization. Advances in X-ray Analysis, 1993, **37**, 37–47.

11 Rigaku, SmartLab Studio II, version 4.3, Rigaku Corporation, Shibuya-Ku-Tokyo, Japan.